

**The influence of test method, conductor profile, and substrate anisotropy
on the permittivity values required for accurate modeling
of high frequency planar circuits**

Allen F. Horn, III
Patricia A. LaFrance
John W. Reynolds
John Coonrod

Introduction

For many years, the design of high frequency electronic circuits was considered an art and numerous design iterations and hand-tuning were expected. However, in the last decade, concomitant with the increasing sophistication of design software and the increasing speeds of personal computers, there is an increasing expectation that the actual circuit performance will mirror the modeled performance. While close agreement of measured and modeled performance is frequently the case, we, as a materials supplier, are occasionally contacted by customers unhappy by the poor agreement between modeled data using the data sheet permittivity and loss values and the actual circuit performance.

As discussed in the present work, depending on the material and design in question, several factors can contribute to a less-than expected agreement between modeled and measured electrical performance.

Form many years, the data sheet permittivity of many high frequency laminates has been reported by the IPC-TM-650 2.5.5.5 clamped stripline test method called for in the IPC-4103 *Specification of Base Materials for High Speed/High Frequency Applications*. In the present work, it is demonstrated that clamped stripline testing on fully etched samples reports a permittivity value that is 5 to 10% lower than measured on microstrip or stripline assemblies with bonded copper foil. We will demonstrate that this discrepancy is in part due to the several micron thick air gap left by the profile of the etched foil as well as a much greater effect of copper foil profile on conductor surface impedance than previously has been documented or accounted for in modeling software.

High profile copper foil results in an increase in surface inductance that alters the propagation constant. The conductor models in many high frequency circuit design software packages do not yet incorporate this effect. This can lead to discrepancies of an additional 15% or greater in the apparent effective permittivity and is particularly evident with high profile copper on relatively thin (less than 0.25 mm) laminates.

Additionally, if not properly accounted for, the anisotropy or directionality of permittivity can result in poorer agreement of measured and modeled performance, particularly with edge-coupled structures and coplanar wave guide circuits.

Basics of Permittivity and loss

The interaction between an electromagnetic field and its environment is described by Maxwell's equations¹:

$$\nabla \cdot \mathbf{D} = \rho_v \quad (1)$$

$$\nabla \cdot \mathbf{B} = 0 \quad (2)$$

$$\nabla \times \mathbf{H} = \partial \mathbf{D} / \partial t + \mathbf{J} \quad (3)$$

$$\nabla \times \mathbf{E} = -\partial \mathbf{B} / \partial t \quad (4)$$

Where \mathbf{E} is the electric field intensity, \mathbf{D} is the electric displacement vector, ρ is charge density, \mathbf{B} is magnetic flux density, \mathbf{H} is the magnetic field strength and \mathbf{J} is the current density vector. While the exact solutions to this set of coupled partial differential equations have been obtained for certain limiting cases, in general, numerical solutions are required,

The following constitutive relationships describe the response in the medium to the applied electromagnetic field:

$$\mathbf{D} = \epsilon \mathbf{E} = (\epsilon' - j\epsilon'') \quad (5)$$

$$\mathbf{B} = \mu \mathbf{H} = (\mu' - j\mu'') \quad (6)$$

$$\mathbf{J} = \sigma \mathbf{E} \quad (7)$$

where by $\epsilon = \epsilon' - j\epsilon''$ is the complex permittivity, $\mu = \mu' - j\mu''$ is the complex permeability and σ is the conductivity.

The low loss circuit substrate materials considered in the present work are non-magnetic ($\mu = \mu$ of free space and $\mu'' = 0$) and non-conductive ($\sigma = 0$), so we will confine our attention to ϵ .

When an electric field is applied to a dielectric material, the field interacts with polar moieties in the material to impose a net electric dipole moment, which augments the total displacement flux that would be experienced in free space, \mathbf{D} . The additional polarization due to the material is a vector \mathbf{P} and in the presence of a dielectric material:

$$\mathbf{D} = \epsilon_0 \mathbf{E} + \mathbf{P} \quad (8)$$

The dielectric materials used for high frequency circuit laminates, and indeed, most dielectric materials are "linear dielectrics," meaning that \mathbf{P} is linear with applied voltage so:

$$\mathbf{P} = \epsilon_0 \chi \mathbf{E} \quad (9)$$

Where χ is the electric susceptibility and is a complex variable, encompassing both the storage and dissipative elements of the dielectric material's interaction with the electric field.

Thus, the displacement flux including material effects is written

$$\mathbf{D} = \epsilon_0 \mathbf{E} + \mathbf{P} = \epsilon_0 (1 + \chi) \mathbf{E} = \epsilon \mathbf{E} \quad (10)$$

$$\epsilon = \epsilon' - j\epsilon'' = \epsilon_0 (1 + \chi) \quad (11)$$

where ϵ , is the material's complex permittivity and ϵ' and ϵ'' are the real (storage) and imaginary (dissipative) parts respectively.

For computational and reference convenience purposes, the real part of the material's permittivity relative to that of free space, ϵ_R is most commonly used where

$$\epsilon_R = \epsilon' / \epsilon_0 \quad (12)$$

The imaginary part is usually expressed as the loss tangent, $\tan(\delta)$, or dissipation factor, DF, where

$$\tan(\delta) = \text{DF} = \epsilon'' / \epsilon' \quad (13)$$

As long as the values are relatively low (<0.02), the $\tan(\delta)$ is the fraction of the electromagnetic energy in a fully developed plane wave dissipated in the dielectric per wavelength traveled.

If the frequency range of 100 MHz to 300 GHz, the majority of the interaction between an electric field and a polymeric material is through rotation and displacement of the dipoles within the polymer². The internal dipole displacement contributes to ϵ_R' and the molecular friction due to the dipole rotation contributes to the $\tan(\delta)$.

Thus, apolar materials where the constituent atoms are similar in electronegativity, such as hydrocarbon polymers, polyethylene, polypropylene, and polystyrene exhibit a low relative permittivity and $\tan(\delta)$ since there is comparatively little interaction of the electric field with the material.

Polar materials, such as epoxy, comprise atoms of differing electronegativity such as carbon and oxygen and exhibit an internal dipole moment. These polar moieties are more easily rotated in the alternating electric field, giving rise to a higher permittivity and higher $\tan(\delta)$.

However, some materials with large electronegativity differences between the constituent atoms, such as the carbon and fluorine in polytetrafluoroethylene (PTFE)

exhibit very low permittivity and loss. This is due to the PTFE polymer's morphology and repeat unit symmetry that results in a very small net repeat unit dipole moment.

Permittivity measurements for high frequency laminate quality control

Stable manufacturing of many microwave circuit devices requires a tight ϵ_R control. Device manufacturers often want the total of both batch-to-batch and within-sheet variation to be less than 0.5%. Manufacturers, both of devices and laminates require a "precise" test method to ensure repeatability. To be able to specify the ϵ_R value to a precision of $\pm 0.5\%$ requires a 95% confidence limit of the test method of better than about $\pm 0.1\%$.

The microwave circuit laminate manufacturer needs a fast, precisely repeatable test method that uses small relatively thin planar samples and measures the ϵ_R in the z-axis (thickness direction). These requirements preclude many common material test methods. With many test methods, such as split post dielectric resonators, and cavity or waveguide perturbation, the calculated ϵ_R depends linearly on the volume or thickness of the samples. With thin laminates, it is problematic to routinely measure thickness to the required $\pm 0.1\%$ accuracy.

Due to the mixed dielectric medium of air and the circuit substrate, microstrip resonators or transmission lines require either resorting to a correlation or field solver to calculate the substrate ϵ_R from the measured circuit performance and the result will vary with the anisotropy of the ϵ_R of the material.

Stripline resonance testing eliminates the above concerns. Precise knowledge of the substrate thickness is not required and since the dielectric medium is homogeneous, accounting for the effect of a mixed medium is unnecessary.

Based largely on the shortcomings of the alternative methods, clamped stripline resonance has become a high frequency laminate industry standard test for ϵ_R and DF at X-band.

Clamped stripline test methods

IPC- TM-650 2.5.5.5c Stripline permittivity at X-band

The major manufacturers of copper clad high frequency circuit laminates widely use the IPC-TM-650 2.5.5.5c "Stripline test for dielectric constant and dissipation factor at X-band test." The detailed test method description is available for free download at the IPC web site, www.ipc.org. This "clam-shell" design clamped stripline test fixture (figure 1) is designed to measure the complex dielectric constant of fully etched circuit substrate by a resonance technique.

The fixture is designed to accept coupons of 1.3 mm thickness for materials with ϵ_R values of greater than 6.0 and 1.5 mm for materials with ϵ_R values less than 6.0. A 0.2 mm thick "pattern card" made of a material with the same ϵ_R value as the material under test is printed with the loosely coupled 20 ohm resonator and 50 ohm probe lines on one side and etched free of copper on the other. The resonator length is sized such that 4th node resonance will occur at approximately 10 GHz.

The two fully etched coupons are placed on either side of the pattern card and the fixture is closed under a constant force and a frequency sweep is run with a network analyzer. The ϵ_R is calculated as

$$\epsilon_R = (n c / 2 f_r (L + \Delta L))^2 \quad (14)$$

where n is the peak node number, c is the speed of light, f_r is the peak resonant frequency, L is the resonator length, and ΔL is the correction for fringing capacitance which is close in value to the dielectric thickness, as discussed in detail in the test method.

The X-band clamped stripline method has proven to be quick and repeatable and an excellent tool for quality control. However, each fixture is limited to a narrow range of ϵ_R and sample thickness.

Historically, designers using soft PTFE-based circuit laminates have confirmed good agreement between the measured and modeled performance of bonded stripline and microstrip assemblies using the ϵ_R values from the clamped stripline test. In more recent years, it has become clear that this test method understates the ϵ_R values of high ϵ_R laminates and rigid laminates.

IPC- TM-650 2.5.5.5.1c Stripline permittivity to 14 GHz

This related clamped stripline test, referred to as the “long stripline” (LSL) method, is a more versatile method with a single fixture allowing a wide range of ϵ_R and thickness values. Samples are 25.4 mm wide by “length” where the length may be 51 mm, 76 mm, 152 mm, and 305 mm. The laminate samples are clamped between thick copper bars, backed up by heavy steel bars that maintain a constant pressure along the length of the sample (figure 2).

The signal is capacitively coupled from the center conductor of RG-405 coaxial cable that is held in a self-centering, micrometer adjustable fixture. The distance between the coax center conductor and the resonator can be increased to maintain the desired loose capacitive coupling at higher frequencies. With the 152 mm length sample and FR4 with an ϵ_R value of about 4, the fundamental node occurs at about 500 MHz and measurements can generally be made to about 14 GHz. The ϵ_R is calculated at each resonant frequency from (14) without the fringing capacitance correction since the resonators are long compared to the sample thickness.

Several configurations of samples can be tested by the LSL method (figure 3). Type A samples are etched free of the copper foil. Both conductors and ground planes are made from smooth rolled copper foil, with the conductor width chosen to achieve an impedance of about 20 ohms. Thus, all four copper-dielectric interfaces are clamped and may contain minute air gaps. The type B samples have copper foil ground planes left intact. The appropriate width conductor is etched into the foil of one half of the clamped assembly with the inner side of the second half is etched free of copper. Type B samples

have three of the four interfaces bonded, and one interface adjacent to the resonator is clamped. Type D samples are bonded, eliminating the presence of air gaps.

Microstrip differential phase length measurements

The microstrip configuration effective permittivity, ϵ_{eff} , of 50-ohm transmission lines on 0.5 mm laminate was calculated from the differential phase length. The phase length of two different lengths of transmission line held in an Intercontinental Microwave WK-3003-D substrate fixture was measured with a HP-8510B network analyzer from 1 to 20 GHz.

$$\Phi = 2\pi f \frac{\sqrt{\epsilon_{\text{eff}}}}{c} L \quad (15)$$

where Φ is the phase length and L is the physical length of the transmission line.

To remove the electrical length of the fixture, we divide the difference in phase length by the difference in physical length of the two transmission lines to yield the differential phase length.

$$\Delta\Phi = 2\pi f \frac{\sqrt{\epsilon_{\text{eff}}}}{c} \Delta L \quad (16)$$

Equation 16 is rearranged to calculate the effective permittivity of the microstrip circuit.

$$\epsilon_{\text{eff}} = \left(\frac{\Delta\Phi c}{2\pi f \Delta L} \right)^2 \quad (17)$$

and laminate ϵ_R was calculated from the ϵ_{eff} value and the physical dimensions of the transmission line using the method of Hammerstad and Jensen [].

Materials and sample preparation

The seven materials tested are listed in table 1. All PTFE samples were 152 mm x 25.4 mm x 0.63 mm thick. The FR4, RO4003C™, and RO4350B™ laminate samples were 152 mm x 25.4 mm x 1.52 mm thick. The nominal ϵ_R value by the X-band stripline method is included in the material ID for each sample except the FR4.

FR4 is an epoxy resin reinforced with 40-60 weight % woven glass fabric. The Rogers RO4000® materials consist of a hydro-carbon (HC) resin that is highly filled with fused amorphous silica and coated onto a considerably lower weight of glass fabric than the FR4. The RO3003™, RO3006™, and RO3010™ laminates samples are particulate-

filled PTFE composites with no glass reinforcement. The filler is a mix of fused amorphous silica and titanium dioxide with the ratio chosen to yield the desired ϵ_R value

The type A samples were fully etched and assembled in the clamped stripline configuration using the smooth rolled copper strips. The resonator strips were 3.2 mm wide.

We also etched 3.2 mm wide resonators in the type B samples using material from the same laminate immediately adjacent to the type A samples. Solid ground planes were left intact on the opposite side.

The type D samples were prepared by bonding the type B samples after testing. The FR4, and HC samples were bonded using the appropriate “pre-preg” and the manufacturers’ suggested lamination conditions. The PTFE samples were “fusion bonded” (i.e., laminated above the melting point of the PTFE resin with no bonding film) at a temperature of 360°C and a pressure of 80 bar, the approximately lamination conditions used to make particulate filled PTFE composite laminates.

Results

Typical Type D sample results from the LSL test show a relatively flat response of ϵ_R versus frequency for the RO4000 laminate materials and a somewhat greater slope with the FR4 (Figure 4).

Similar curves were generated for type A, B, and D samples for the six materials listed in table 1.

Effect of bonding / air gaps

The average ϵ_R of the three nodes closest to 10 GHz is shown for the three LSL sample types and the microstrip lines are shown in table 2.

One will note that the measured ϵ_R values increase as the number of air gaps between conductor and dielectric are reduced going from sample types A to B to D for all materials.

The RO3035™ laminate sample exhibits a 2% difference in ϵ_R between the type A (clamped) and type D (bonded) samples. The effect of the air gaps is small since this material is both relatively soft and has a low ϵ_R .

The RO4003C™ and RO4350B laminate samples exhibit a somewhat more significant 3 to 3.7% increase in ϵ_R from the clamped to bonded samples. While low in ϵ_R , the rigidity of these materials apparently allows more air to be entrapped at the interface.

Similar to the HC materials, the FR4 sample also exhibits an increase in ϵ_R of about 3.5% between type A and type D samples.

The RO3006 and RO3010 laminates exhibit an increase of 6.4% and 9.0% respectively when the type D bonded samples are compared to the clamped type B samples.

These data demonstrate that the major cause for the low permittivity measured by clamped stripline tests is due to the presence of air at the interface left behind by the etching of the copper foil cladding. An exaggerated sketch is shown in figure 5.

Rogers Corporation has chosen to add a “design DK” (permittivity) value to the data sheet of the rigid or high permittivity laminates that are susceptible to air gap discrepancy. The design DK value is extracted from the differential phase length measurements made on 0.5 mm and 0.625 mm microstrip assemblies. Our experience with customers is that the design DK values frequently result in good agreement of modeled and measured data in both microstrip and stripline assemblies. However, there are additional complications of conductor effects and permittivity anisotropy that are discussed below.

Conductor effects

The majority of planar circuit substrates are clad with one of three types of commercially available copper foil specifically manufactured for that purpose: Rolled/Annealed, (RA), Electro-deposited (ED) and reverse treated (RT). The foils are treated by the foil manufacturers with different types of treatments to improve and preserve adhesion to different types of circuit substrates. Historically, high profile (“rough”) foils have been used to increase adhesion to the dielectric material while lower profile foils are used to improve etch definition or reduce conductor loss.

The surface profiles in the current work have been characterized using a Veeco Metrology Wyko NT1100 optical profiling system. The instrument’s operation is based on white light interferometry. This non-contact method generates a three dimensional image of the surface topography with a resolution of about 1 nm in a 1 mm square area. The profile can be characterized by a wide variety of different statistics, including r_z , the peak-to-valley roughness, r_q (or R_{RMS}), the root-mean-square roughness, and the surface area index. R_{RMS} is most widely used in characterizing conductor roughness in high frequency electrical applications.

RA (rolled/annealed) foil is produced from an ingot of solid copper by successively passing it through a rolling mill. After rolling, the foil itself is very smooth, with an RMS profile (R_{RMS}) of 0.1 to 0.2 μm . For printed circuit substrate applications, the foil manufacturer additively treats the rolled foil, increasing the R_{RMS} to 0.4 to 0.5 μm on the treated side.

ED (electro-deposited) foil is produced by plating from a copper sulfate solution onto a slowly rotating polished stainless steel drum. The “drum side” of ED foil exhibits an

R_{RMS} of about 0.1 to 0.2 μ , similar to untreated RA foil. The profile of the “bath side” of the plated foil is controlled by the plating conditions, but is considerably higher in profile than the drum side. The ED foil manufacture generally applies a further plated treatment to the batch side of the foil for improved adhesion and chemical compatibility with the intended dielectric material. ED foils have historically been manufactured with R_{RMS} values in the range of 1 to 3 μ . The 2500X SEM photograph (figure 6) visually demonstrates the difference between a high profile (3 μ m RMS) ED foil and a low profile (0.5 μ m RMS) RA foil.

It has long been known that conductor roughness increases conductor loss at higher frequencies. In 1949, S. P. Morgan⁴ published a paper numerically modeling the effect of regular triangular and square patterned grooves in a conductor surface on the conductor loss at different frequencies. As the skin depth of the signal approaches the height of the grooves, the conductor loss increases. With grooves with an aspect ratio of about 1:1, the maximum increase of a rough conductor is a factor of two for a signal traveling perpendicular to the grooves and considerably small for a signal traveling parallel. A simple explanation of the mechanism is that the small skin depth signal must travel along the surface of the rough conductor, effectively increasing the path length and conductor resistance.

The Morgan correlation was adapted into an automated microstrip insertion loss and impedance calculation described by Hammerstad and Jensen (H&J). The correlation is incorporated as a multiplicative correction factor K_{SR} to the attenuation constant calculated for a smooth conductor.

$$\alpha_{cond, rough} = \alpha_{cond, smooth} \cdot K_{SR} \quad (18)$$

where $\alpha_{cond, smooth}$ is the attenuation constant calculated for a smooth conductor and

$$K_{SR} = 1 + \frac{2}{\pi} \arctan \left(1.4 \left[\frac{R_{RMS}}{\delta} \right]^2 \right) \quad (19)$$

Where R_{RMS} is the RMS value of the conductor roughness and δ is the skin depth. It should be noted that both $\alpha_{cond, smooth}$ and K_{SR} are functions of frequency. When the ratio of R_{RMS}/δ is small, as with a smooth conductor or at low frequencies where the skin depth is large, the value of K_{SR} is close to one. As the ratio becomes large as with higher profile conductors and higher frequencies, the value of K_{SR} approaches two (figure 7). This correlation predicts a “saturation effect,” i.e., that the maximum effect of the conductor roughness would be to double the conductor loss. This result also implies that the conductor loss for a lower profile foil will eventually approach that of a rough foil as frequency increases.

However, more recent theoretical work by Tsang et al.⁵ and Huray et al.⁶ have shown that this saturation effects should not occur, and that increase in conductor loss of greater than a factor of two can be caused by higher profile conductors.

The present authors found only two recent papers directly addressing the effects of conductor profile on the phase constant. Ding et al⁷ have conducted modeling of wave propagation in a randomly rough parallel plate waveguide. They state “the phase angle of the coherent wave shows that the rough waveguide exhibits more phase shift than a smooth waveguide corresponding to an increase in phase constant,” though the magnitude of the effect is not quantified.

Deutsch et al⁸ measured the relative dielectric constant, ϵ_R , of 0.0025” and 0.010” thick samples of FR4 laminate clad with rough and smooth copper foil using the “full sheet resonance” test method⁹. The calculated ϵ_R of the thin substrate clad with the rough foil was approximately 15% higher than that of the same thickness substrate with smooth foil. The increase in calculated ϵ_R of the thin substrate clad with the smooth foil was considerably lower. Modeling with both a three dimensional, full-wave electromagnetic field solver and a two dimensional code that included the detailed profile of the conductors confirmed the approximate magnitude of the measured results. The authors attribute the increase in calculated ϵ_R to the increase in inductance caused by the conductor profile. Both the models and measured data also show an increase in dispersion (frequency dependence of ϵ_R) that is also caused by the effect of conductor profile on inductance

Horn, III et al^{10, 11}, experimentally measured the differential insertion loss and differential phase length of 50 ohm transmission lines on Rogers ULTRALAM® 3000 LCP laminates clad with copper foils with roughness values ranging from 0.4 μ m to 3.0 μ m RMS. The ULTRALAM LCP laminate was chosen since it is an unreinforced pure polymer and there is no question that the material’s permittivity could vary with composition or thickness.

As is discussed below, reference experimentally quantifies both the larger than previously predicted increase in conductor loss and the previously generally unknown (with the exception of references 7 and 8) effect of conductor roughness on the propagation constant.

Insertion loss results up to 50 GHz (figure 8) for copper foils with profiles of 0.5, 0.7, 1.5, and 3.0 μ m on the 0.004” thick LCP dielectric material show a number of interesting features. The measured data for the 0.5 μ m nearly match the line calculated for smooth foil using the method of H&J and the MWI impedance calculator. The line calculated for conductor profile of 1.5 μ m (white line) match the measured data at low frequencies, but at frequencies higher than about 20 GHz, the measured data are substantially higher in loss than the calculated. The same general features are exhibited by the 3 μ m profile data measured and calculated data.. The calculated line for 3 μ m (black diamonds) matches the measured data up to about 10 GHz. At higher frequencies, the measured data exhibit substantially higher insertion loss than the calculated line.

These data clearly show that saturation does not occur, at least up to frequencies of 50 GHz and that the effect of conductor profile is larger than predicted by the Morgan correlation at frequencies above 10 GHz.

The effective dielectric constant of the microstrip circuit, ϵ_{eff} , was calculated from the differential phase length from 8 to 50 GHz, and smoothed with a 4th order polynomial fit and the data are plotted for the four copper types in figure 9. There is a substantial effect of the copper profile on the ϵ_{eff} value. For the 0.5 μm profile foil, the ϵ_{eff} value is about 2.36 at 10 GHz while the value for the 3 μm profile foil is 2.66 at the same frequency. Clearly, the propagation constant is strongly affected by the conductor profile.

Additional measurements described in reference were done comparing the effect of high (3.0 μm RMS) and low (0.4 μm RMS) profile copper foils on the propagation constant in 50 ohm transmission lines on LCP laminates ranging from 0.1 mm to 0.5 mm in thickness. The “substrate permittivity”, ϵ_{sub} , was calculated using the method of H&J from the ϵ_{eff} measured by differential phase length. A plot of the 5-35 GHz average ϵ_{sub} (figure 10) versus laminate thickness shows that the effect of the smooth copper on propagation constant is small, while the use of the high profile foil substantially increases the apparent ϵ_{sub} by about 15% as the laminate thickness decreases (figure 11).

To our knowledge, most conductor models used in high frequency circuit modeling software do not encompass this effect of conductor roughness on propagation constant. One exception is Sonnet® Software, in which the conductor model includes an increase in surface inductance that has been shown to predict both an insertion loss and propagation constant that agrees with measured values on a wide range of materials and laminate thicknesses.

We recommend that the engineer interested in accurate modeling ascertain if the software’s conductor model accounts properly for the effect of conductor roughness on both the loss and propagation constant. If not, other methods will be necessary to get good agreement between measured and modeled data, particularly when high profile copper foil and thin dielectric laminates are used.

An alternative method to get models using the traditional conductor models to predict measured performance is to include the conductor effect on propagation constant in the apparent ϵ_{sub} of the material. A plot of the apparent ϵ_{sub} of Rogers RO4003C and RO4350B laminates with the standard high profile copper foil shows the increase in ϵ_{sub} input to the software necessary to get good agreement between modeled and measured performance if a traditional conductor model is used (figure 12). The same plot for and RO4003C and RO4350B LoPro™ laminates with a low profile copper foil actually show a slight decrease in the value of ϵ_{sub} as laminate thickness decreases.

Composite Mixing Rules and Anisotropy

As described by Neelakanta¹², the mixing rules that predict the properties of a composite, such as thermal conductivity, dielectric constant, or modulus, based on those of its components depend highly on the spatial arrangement of the components, as well as the volume fraction of each component.

The parallel arrangement of materials (figure 13a) leads to a simple mixing rule in which the composite property is the sum of the component properties weighted for their volume fraction in the composite. In the case of the ϵ_R of a composite with N components

$$\epsilon_{Rcomposite} = \sum_{i=1}^N v_i \epsilon_{Ri} \quad (20)$$

where v_i is the volume fraction of component i and ϵ_{Ri} is the permittivity of that component. The parallel arrangement is the upper bound for ϵ_R , as well as dielectric constant and modulus. The parallel arrangement is a reasonable model for the in-plane properties of woven glass fabric reinforced resin composites like epoxy-glass FR4 laminate or woven glass-PTFE high frequency laminate.

The series arrangement (figure 13b) leads to the lower bound for a composite's thermal conductivity, permittivity, and modulus. The ϵ_R of a series composite is given by

$$\epsilon_{Rcomposite} = 1 / \sum_{i=1}^N v_i \epsilon_{Ri}^{-1} \quad (21)$$

The z-axis (through plane) properties of resin impregnated woven glass fabric composites are examples of composite material properties that are very nearly approximated by the series model.

Over the years, a number of models of varying degrees of complexity have been proposed to describe the behavior of dispersed phase composites (figure 13c). A major consideration is accounting for the proportion of series and parallel character of each phase. Obviously, the continuous phase exhibits some degree of parallel character due to its continuity. A convenient equation that often yields remarkably good agreement given its simplicity is the logarithmic mixture law¹³ also known as Lichtenecker's rule given by

$$\log(\epsilon_{Rcomposite}) = \sum_{i=1}^N v_i \log(\epsilon_{Ri}) \quad (22)$$

A dispersed phase composite is an approximation of a ceramic powder filled polymeric material. The logarithmic mixing rule predicts an isotropic permittivity which is, in fact observed, if the dispersed filler particles are spherical.

However, with irregularly shaped filler particles, the sheet forming process will often selectively align the particles, resulting in surprisingly high values of anisotropy.

In the most general case, the permittivity of an anisotropic material will be described by a nine element tensor.

$$\begin{pmatrix} D_x \\ D_y \\ D_z \end{pmatrix} = \begin{pmatrix} \epsilon_{xx} & \epsilon_{xy} & \epsilon_{xz} \\ \epsilon_{yx} & \epsilon_{yy} & \epsilon_{yz} \\ \epsilon_{zx} & \epsilon_{zy} & \epsilon_{zz} \end{pmatrix} \begin{pmatrix} E_x \\ E_y \\ E_z \end{pmatrix} \quad (23)$$

However, as a practical matter, the off-diagonal elements such as ϵ_{xy} (quantifying the displacement flux in the x direction arising from the electric field in the y-direction) are insignificant in common dielectric materials and it is sufficient to only consider the diagonal elements

$$\begin{pmatrix} D_x \\ D_y \\ D_z \end{pmatrix} = \begin{pmatrix} \epsilon_{xx} & 0 & 0 \\ 0 & \epsilon_{yy} & 0 \\ 0 & 0 & \epsilon_{zz} \end{pmatrix} \begin{pmatrix} E_x \\ E_y \\ E_z \end{pmatrix} \quad (24)$$

Furthermore, in circuit laminates, ϵ_{xx} and ϵ_{yy} rarely differ significantly from each other and for modeling purposes, only the z-axis (out of plane) value, ϵ_{zz} , and x-y plane (in-plane) value, ϵ_{x-y} are used. Many practical test methods, such as resonator perturbation, by nature, measure the in-plane average permittivity, ϵ_{x-y} , and cannot resolve the individual components, ϵ_{xx} and ϵ_{yy} .

Experimental measurements of laminate anisotropy

“Two resonator” test method of Dankov

In *Dielectric Anisotropy of Modern Microwave Substrates*, Dankov^{14, 15} describes a “two resonator” test method using fully etched samples that measures the in-plane and z-axis permittivity of high frequency circuit laminates. The two resonator test method exploits the fact that different resonant cavity designs and different propagation modes can be chosen to obtain the **E**-field either in-plane or out-of-plane with the sample to be measured. Dankov demonstrates the test method to be accurate to within 0.5% or better for ϵ_{x-y} and ϵ_{zz} and also measures the expected near-zero anisotropy of pure PTFE polymer sheet, as well as polyolefin and polycarbonate materials. With the resonator test methods, the intensity of the electric field is uniform throughout the thickness of the laminate, so it measures the true bulk values of the ϵ_{zz} and ϵ_{x-y} of the laminate. It is interesting to compare Dankov’s results with the clamped stripline resonator test method and with the simple mixing rules. Selected data from reference 15 taken at about 12 GHz are shown in table 3. The % anisotropy is defined as:

$$\Delta A\% = 100 * (\epsilon_{xy} - \epsilon_{zz}) / (\epsilon_{xy} + \epsilon_{zz}) \quad (22)$$

Rogers RO3003 laminate is a composite of PTFE and a dispersed filler comprised predominantly of ground fused silica powder. The fused silica is irregular in shape and has an ϵ_R of about 3.8 compared to the ϵ_R of 2.05 for PTFE. A dispersed-phase

composite with relatively small difference in ϵ_R of the filler and resin would be expected to be low in anisotropy, consistent with Dankov's measured anisotropy of 1.0%.

Rogers RO3203™ laminate comprises plies of PTFE-silica powder composite with about 15 volume% woven glass fabric to increase the laminate stiffness. The addition of the higher permittivity ($\epsilon_R = 6.5$) glass fabric increases the in-plane permittivity, resulting in a greater degree of anisotropy, consistent with Dankov's measured value of 7.2%.

Nelco® NH9300 laminate is a woven glass fabric-PTFE composite laminate. It is a reasonable approximation of the geometry to consider the composite as alternating sheets of PTFE resin and glass fabric. Thus, in-plane it will exhibit a high degree of parallel character, while out-of-plane, it will be very close to a series arrangement when considering the PTFE and glass fabric. Dankov measures an ϵ_{zz} of 2.82, and an ϵ_{x-y} value of 3.42, resulting in an anisotropy ratio of 19.2%. At 60 volume % PTFE, equation 21 predicts an ϵ_{zz} of 2.82 and equation 20 predicts an ϵ_{x-y} value of 3.83, resulting in a calculated anisotropy of 28%. This hardly constitutes quantitative agreement. However, considering the fact that fabric is not really a continuous solid sheet and therefore exhibits less of a parallel character than implied by equation 20, the simple equations are at least, indicative of the correct trend.

Rogers RO4003C laminate is a three phase consisting of dispersed silica in a hydrocarbon resin, reinforced with a relatively small amount of glass fabric and results in an anisotropy of about 8.3%.

Nelco® NH9338 PTFE-woven glass fabric laminate contains a higher fraction of the glass fabric and a small amount of titanium dioxide to increase the permittivity. As above, the predominantly lamellar arrangement of the glass fabric and PTFE and the relatively large difference in permittivity of the two components results in Dankov measuring a relatively high anisotropy value of 24.6%.

As discussed earlier, Rogers RO3010 laminate is a PTFE-titanium dioxide powder dispersed phase composite with a permittivity value of 10.2 as measured by the clamped stripline method. The titanium dioxide particles are irregular in shape. The permittivity of the titanium dioxide is about 100. Due to the sheet forming process aligning the major axis of the filler particles in an "in-plane" orientation, the measured anisotropy is 14.7%. Rogers TMM® 10i laminate is a hydrocarbon resin material containing a spherical proprietary titanate filler. The use of the physically nearly isotropic particles reduces the measured permittivity anisotropy by more than 50%.

It is also interesting to note that Dankov's ϵ_{zz} values for the Rogers-manufactured materials all agree with the clamped stripline values discussed above to within 1%, with the exception of the TMM10i laminate that exhibits a difference of about 5% between the two test methods. It should be remembered that the two resonator method samples are etched free of copper foil. Thus, similar to the clamped stripline method the resonator method yields ϵ_{zz} values that would be low compared to those measured on microstrip

circuits for materials that are rigid or high permittivity but appear to be in good agreement with the softer, low ϵ_{zz} materials such as RO3003 or RO3203 laminates.

Dual Mode Microstrip Resonator Method

Rautio et al.^{16, 17} have developed a considerably different test method for measuring high frequency laminate ϵ_R anisotropy. As discussed in reference 17, anisotropy most affects the discrepancy between measured and modeled performance when working with edge coupled structures such as band pass filters and differential pair transmission lines. Rautio et al.¹⁷ show that one can achieve a model that accurately predicts the center frequency of a band pass filter with a single isotropic ϵ_R value, but the predicted band width will too narrow. When the anisotropy of permittivity is correctly accounted for, both center frequency and bandwidth can be accurately modeled.

The dual mode microstrip resonator method (“RA resonator” for authors Rautio and Arvas) sample consists of a pair of closely coupled parallel lines etched on a microstrip substrate (figure). The long lines allow measurement from a relatively low frequency and at closely spaced resonant frequencies. Resonant peaks are taken from a sweep of S11 over frequency and the permittivity is extracted using a Sonnet® Software model. The two lines give rise to two resonant modes. The electric field structures are very different between even mode (figure 15a) and odd mode (figure 15.b) resonance. Odd mode coupling between the lines causes the ϵ_{x-y} to be relatively dominant while the even mode coupling to the ground plane accentuates the effect of the ϵ_{zz} .

Dual mode microstrip RA resonator results for several materials at 10 GHz are shown in table 4. Rogers RO4350B laminate is nearly identical in formulation to the RO4003C material, except for the addition of a flame retardant, so anisotropy of the two materials is expected to be similar. Since the RA resonator samples are actual microstrip circuits with the copper foil bonded to the dielectric, the measured ϵ_{zz} values are quite comparable with the bonded stripline or microstrip phase length results presented earlier in table 1.

We were initially quite surprised to discover that the ϵ_{x-y} (in-plane) permittivity values of the woven glass fabric composites was lower than the ϵ_{zz} , contrary to the measurements of the bulk in-plane permittivity of Dankov and the expected values from theory.

However, after some reflection and referring again to figure 15b , it is clear that the magnitude of the **E**-field for the odd mode resonance is greater closer to the surface of the laminate. The higher ϵ_R glass fabric can be many microns from the conductors so the properties of the lower permittivity resin phase dominate the effective ϵ_{x-y} .

This is corroborated by the RA resonator results on the RO3010 laminate. Recalling that this material does not contain glass fabric, but is filled with titanium dioxide of several microns in diameter, its composition is nearly uniform on the scale of the **E**-field all the way to the interface with the conductors. Thus, while the RA resonator value for ϵ_{zz} is

11.0 the in-plane ϵ_{x-y} value of 12.0 is quite similar to the bulk value measured by Dankov. In this case, the bulk ϵ_{x-y} and effective ϵ_{x-y} for tightly edge-coupled structures is the same.

However, with a lamellar composite laminate, the effective ϵ_{x-y} could be different in the same material depending on the degree of coupling between the structures of interest. Tightly coupled structures will exhibit a lower effective ϵ_{x-y} since the \mathbf{E} -field is strongest in the resin-rich surface. Knowing the bulk ϵ_{x-y} for lamellar composite structures could actually lead a designer in the wrong direction.

Conclusions and Recommendations

Clearly, there is no single value for permittivity of a material that will yield good agreement between modeled and measured data for all high frequency circuit design software systems.

The data sheet permittivity values measured by the IPC-TM-650 2.5.5.5 clamped stripline test method in accordance with IPC-4103 high frequency material specification can be 5 to 10% lower than is measured by methods using conductors that are bonded directly to the laminate with rigid or high permittivity materials. Rogers also publishes a recommended “design dielectric constant” based the differential phase length of microstrip transmission lines for these materials where the IPC-TM-650 2.5.5.5 permittivity value does not work well for circuit design.

The effect of conductor profile on the propagation constant needs to be considered, particularly when modeling thin (< 0.5 mm) laminates with higher profile copper foils. The designer should make sure to understand the conductor model that is used by his or her software design package and account for the effect accordingly.

With uniform, particulate filled composite laminates, the bulk ϵ_{x-y} value may be adequate for designing edge coupled structures affected by anisotropic permittivity. However, when designing on lamellar woven glass fabric reinforced composite laminates, the effective ϵ_{x-y} can vary with coupling. Accurate modeling may require some variant of the RA dual resonator method with coupling similar to the final structure.

1. David M. Pozar, *Microwave Engineering*, 2nd edition, J. Wiley & Sons, New York (1998)
2. Chen C Ku & Raymond Liepins, *Electrical Properties of Polymers: Chemical Principles*, Hanser Publishers, Munich (1987)
3. E. Hammerstad and O. Jenson, "Accurate models for microstrip computer aided design," *1980 IEEE MTT-S Int. Microwave Symp. Dig*, pp. 407-409, May 1980.
4. S. P. Morgan, "Effect of surface roughness on eddy current losses at microwave frequencies," *J. Applied Physics*, p. 352, v. 20, 1949
5. L. Tsang, X. Gu, & H. Braunisch, "Effects of random rough surfaces on absorption by conductors at microwave frequencies, *IEEE Microwave and Wireless Components Letters*, v. 16, n. 4, p. 221, April 2006
6. Paul G. Huray, Femi Oluwafemi, Jeff Loyer, Eric Bogatin, & Xiaoning Ye, "Impact of Copper Surface Texture on Loss: A Model That Works," DesignCon 2010 Proceedings, Santa Clara, CA, 2010.
7. R. Ding, L. Tsang, & H. Braunisch, "Wave propagation in a randomly rough parallel-plate waveguide," *IEEE Transactions on Microwave Theory and Techniques*, v. 57, n.5, May 2009
8. Deutsch, A. Huber, G.V. Kopcsay, B. J. Rubin, R. Hemedinger, D. Carey, W. Becker, T Winkel, & B. Chamberlin, p. 311, ., *IEEE Symposium on Electrical Performance of Electronic Packaging*, 2002
9. The Institute for Interconnecting and Packaging Circuits, www.ipc.org, IPC-TM-650 Test Methods Manual, 2.5.5.6
10. A. F. Horn, III, P. A. LaFrance, J. W. Reynolds, J. C. Rautio, *Effect of conductor profile on the insertion loss, phase constant, and dispersion in thin high frequency transmission lines*. DesignCon 2010 Proceedings, Santa Clara, CA, 2010.
11. A. F. Horn, III, J. W. Reynolds, J. C. Rautio, *Conductor profile effects on the propagation constant of microstrip transmission line*, Microwave Symposium Digest (MTT), 2010 IEEE MTT-S International, pp 868-871
12. Neelakanta, P. S., *Handbook of Electromagnetic Materials*, pp. 108-111, CRC Press, New York (1995)
13. Bujard, P., **Proceedings of I-THERM**, IEEE, Los Angeles May 11-13, p. 41 (1988)
14. P. I. Dankov, B. N. Hadjistamov, I. P. Arestove, and V. P. Lecheva, "Measurement of dielectric anisotropy of microwave substrates by two-resonator method with different pairs of resonators," *PIERS Online*, Vol. 5, No. 6, 2009
15. P. I. Dankov, *Dielectric Anisotropy of Modern Microwave Substrates, Microwave and Millimeter Wave Technologies from Photonic Bandgap Devices to Antenna and Applications*, Igor Minin (Ed.), ISBN: 978-953-7619-66-4, InTech, 2010
16. J. C. Rautio and S. Arvas, *Measurement of Planar Substrate Uniaxial Anisotropy*, *IEEE Trans. Microwave Theory and Techniques.*, vol. 57. no.10, pp. 2456-2463, Oct 2009
17. J. C. Rautio, R. L. Carlson, B. J. Rautio, and S. Arvas, *Shielded Dual-Mode Microstrip Resonator Measurement of Uniaxial Anisotropy*, *IEEE Trans. Microwave Theory and Techniques.*, vol. 59. no.3, pp. 748-754, 2011

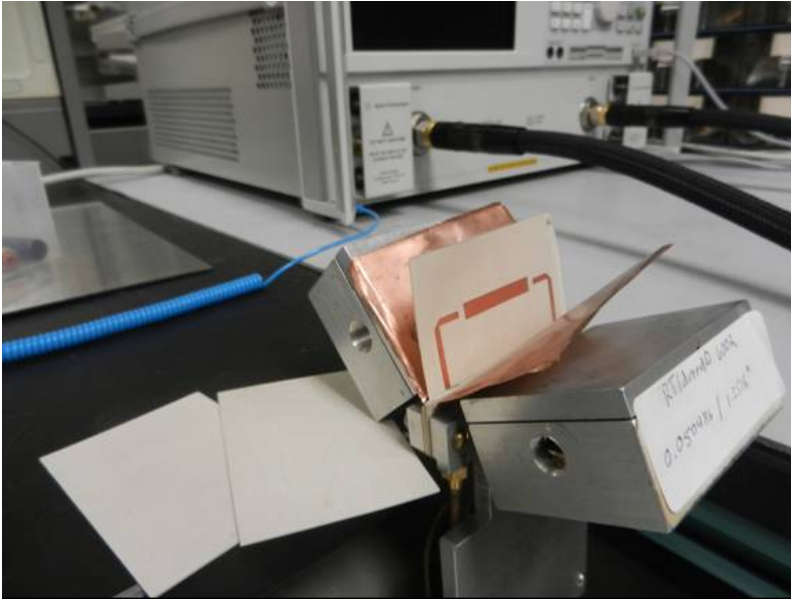


Figure 1: IPC-TM-650 2.5.5.5 clamped stripline test fixture. The two 1.5 mm fully etched coupons are inserted on either side of the patterned resonator card and the fixture is closed to form a stripline circuit

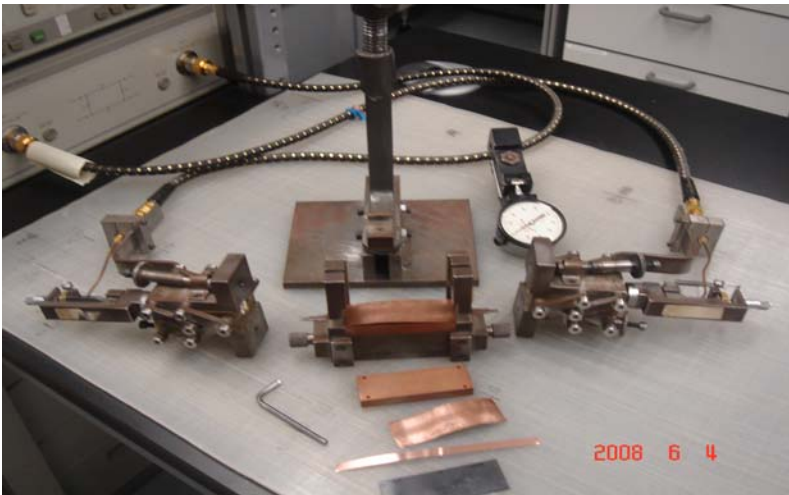


Figure 2. IPC-TM-650 2.5.5.5.1 stripline permittivity to 14 GHz Etched dielectric to be assembled with copper foil to form a clamped stripline assembly.

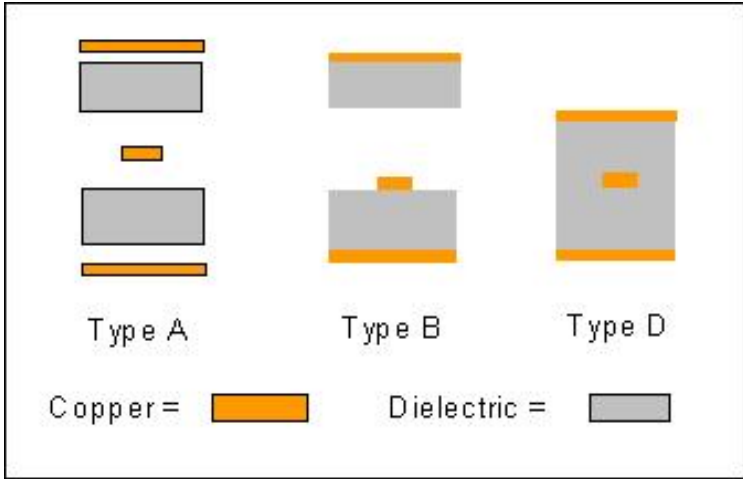


Figure 3. End view of LSL sample configurations

Material	Description
FR4	Epoxy-fiberglass laminate
RO4003™	Hydrocarbon-silica woven glass laminate
RO4350™	Hydrocarbon-silica woven glass laminate
RO3035™	Commercial grade PTFE-particulate laminate
RO3006™	Commercial grade PTFE-particulate laminate
RO3010™	Commercial grade PTFE-particulate laminate

Table 1

Material	10 GHz Permittivity Values			
	Type A	Type B	Type D	Microstrip
FR4	4.09	4.17	4.23	4.30
RO4003™	3.46	3.52	3.57	3.61
RO4350™	3.50	3.57	3.63	3.66
RO3035™	3.54	3.54	3.61	3.62
RO3006™	6.11	6.27	6.53	6.57
RO3010™	10.14	10.64	11.05	11.00

Table 2

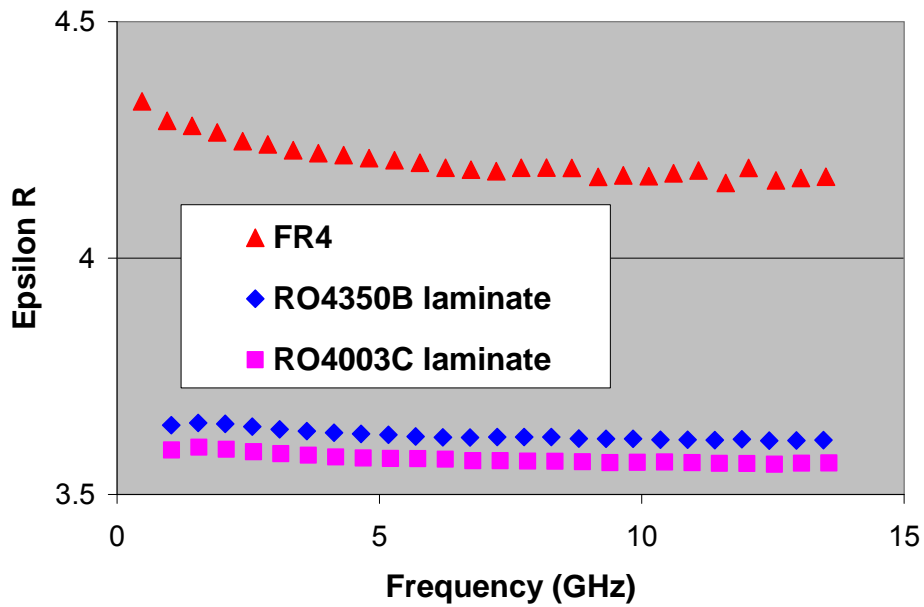


Figure 4. Permittivity versus frequency for selected Type D laminate samples measured by LSL.

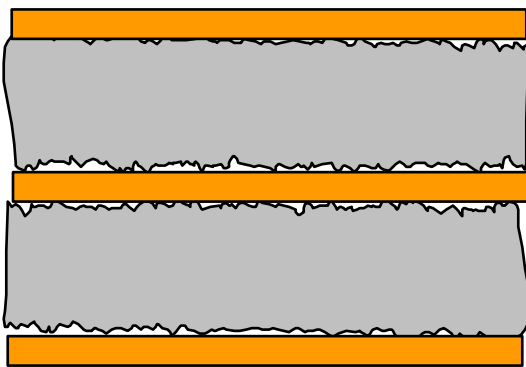


Figure 5. Exaggerated cutaway view of air gaps with fully etched sample in a clamped stripline assembly.

2500X SEM photos of treated copper foil

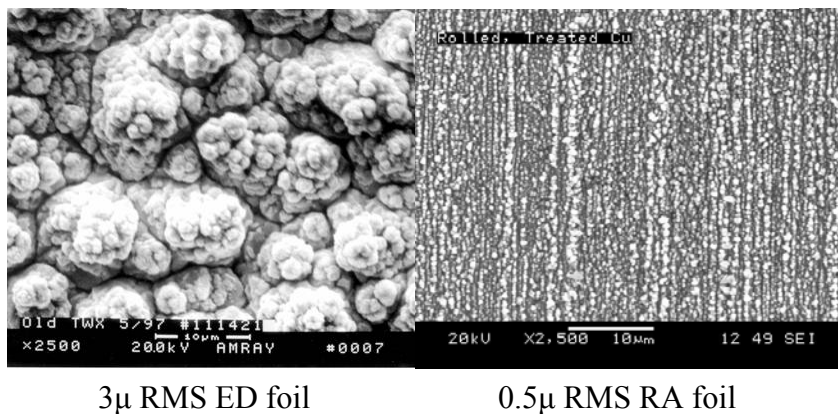


Figure 6. Copper foil images

Conductor roughness attenuation factor vs. Frequency
RMS profile as a parameter

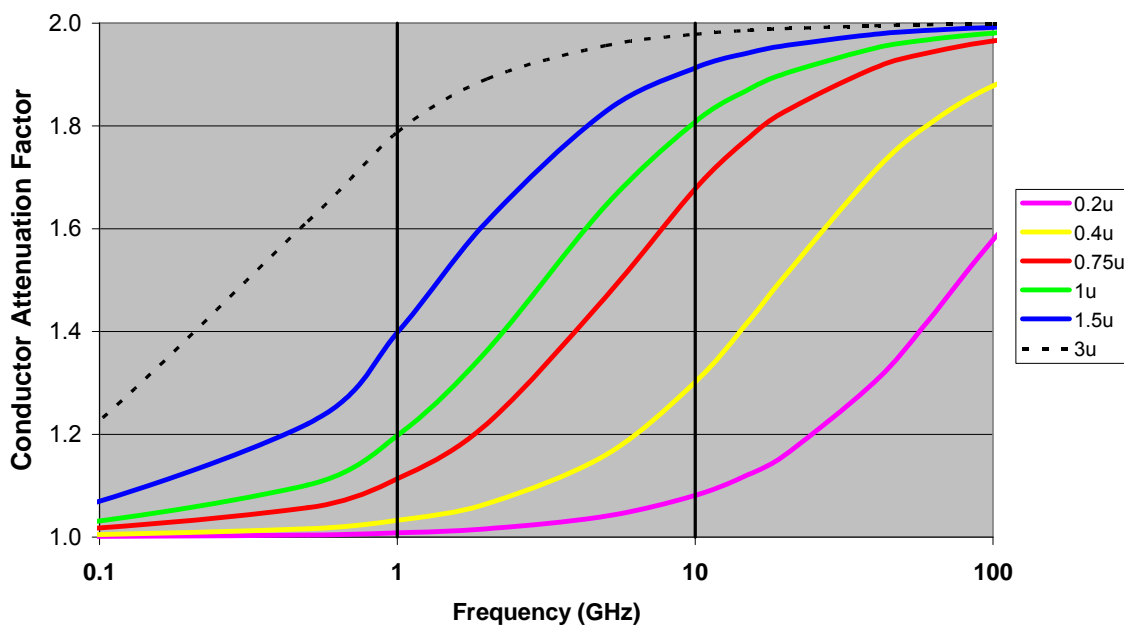


Figure 7. H&J/Morgan-calculated conductor attenuation factor, K_{SR}

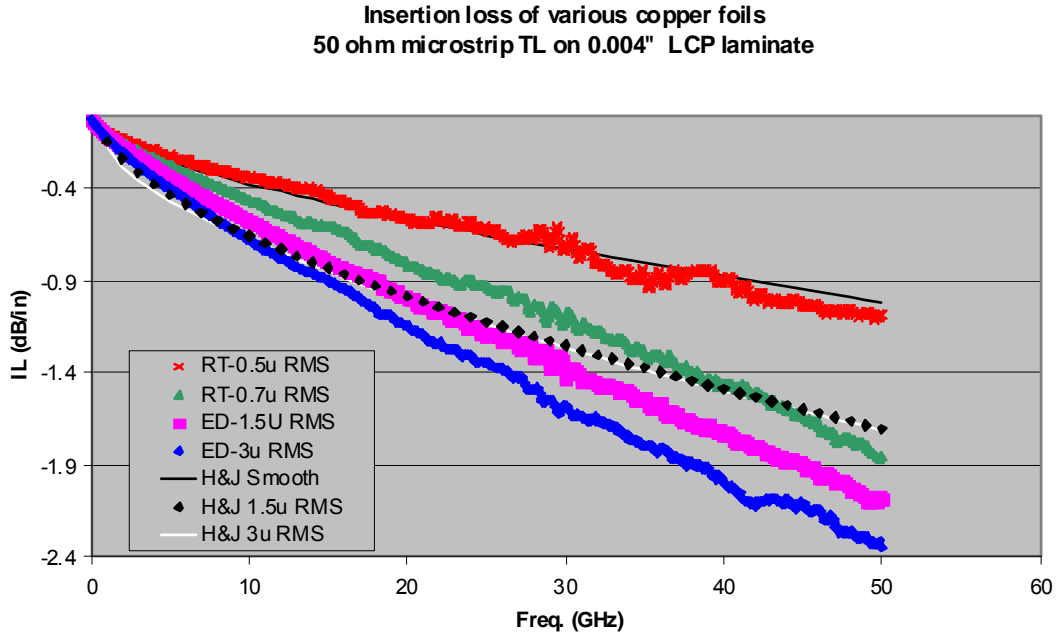


Figure 8. Data of reference 10

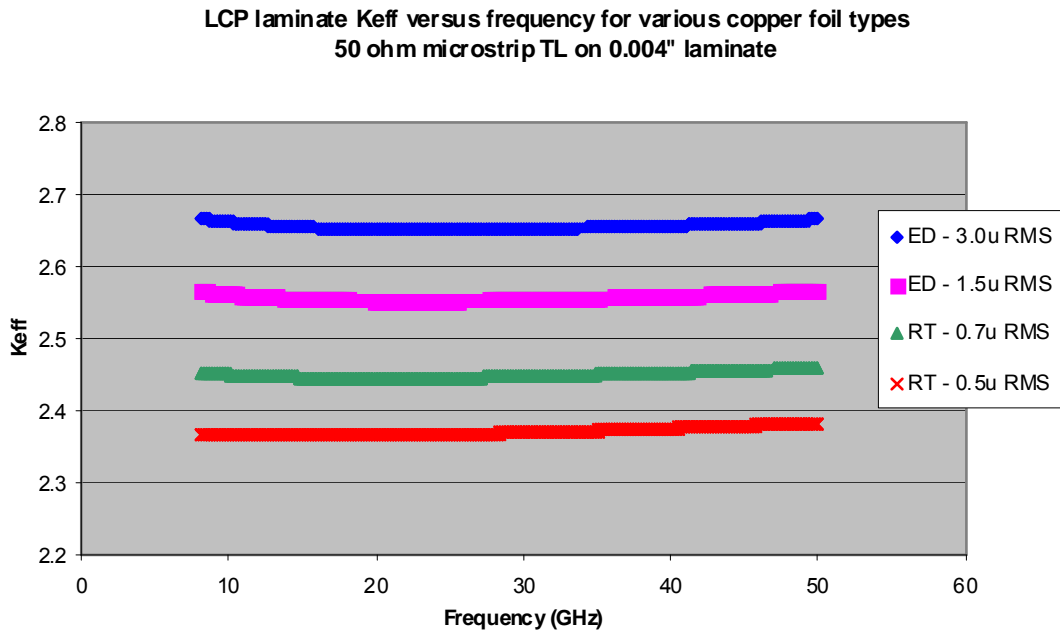


Figure 9. Data of reference 10

Calculated Eps[R] of LCP laminate with 0.5u RMS RA foil
Effect of laminate thickness

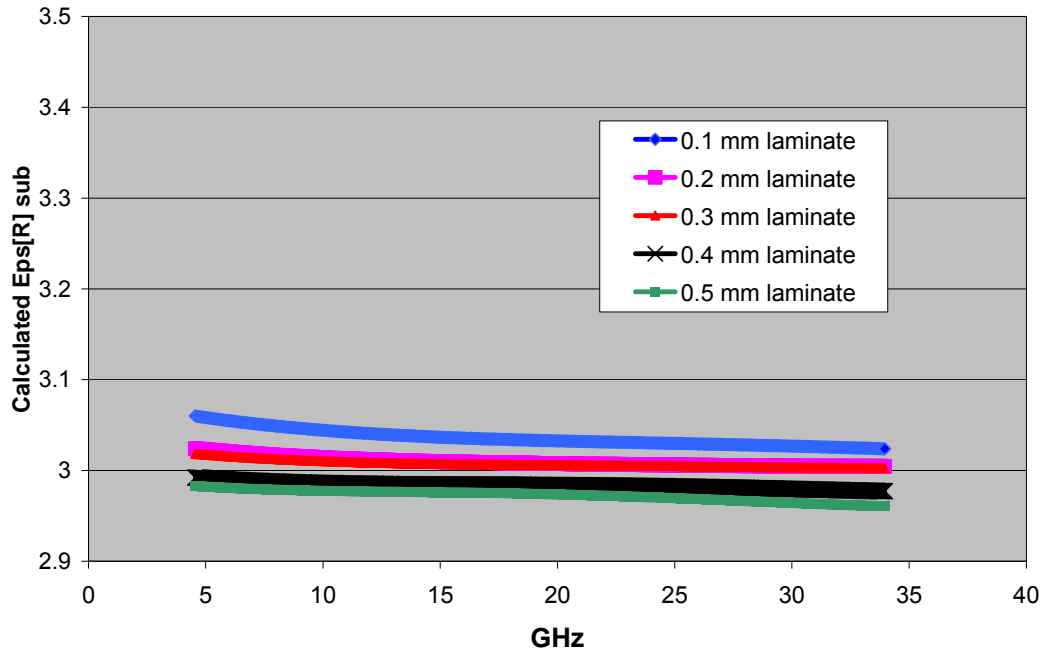


Figure 10. Data of reference 10

Calculated Eps[R]sub of LCP laminate with 3u RMS ED foil
Effect of laminate thickness

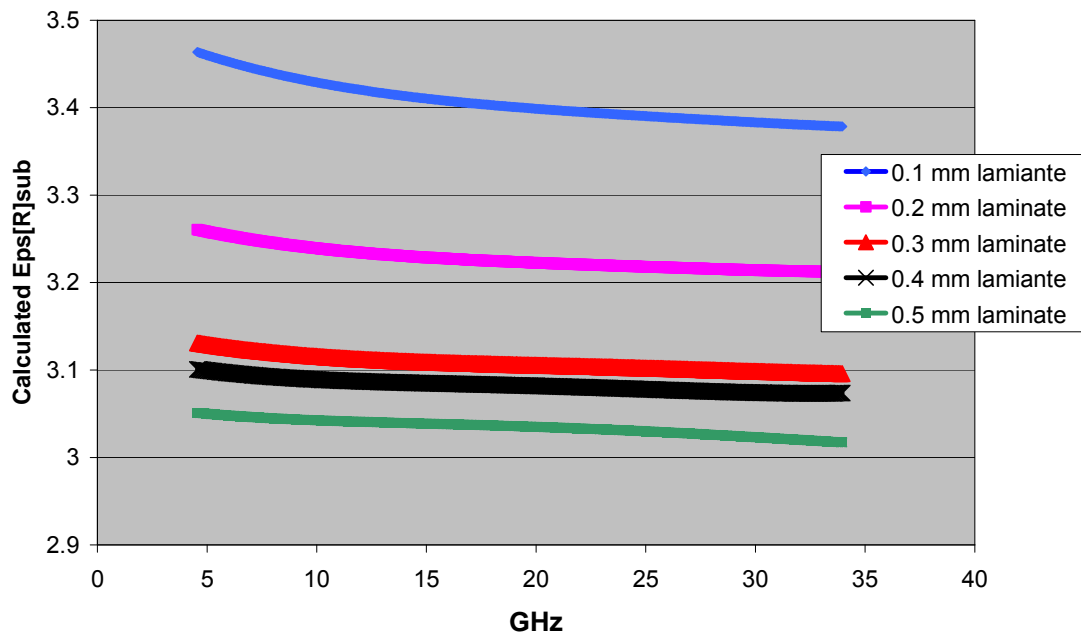


Figure 11. Data of reference 10

**Average Eps[R] sub (8-50 GHz) versus thickness
for RO4000® substrates with LoPro™ and standard copper foils**

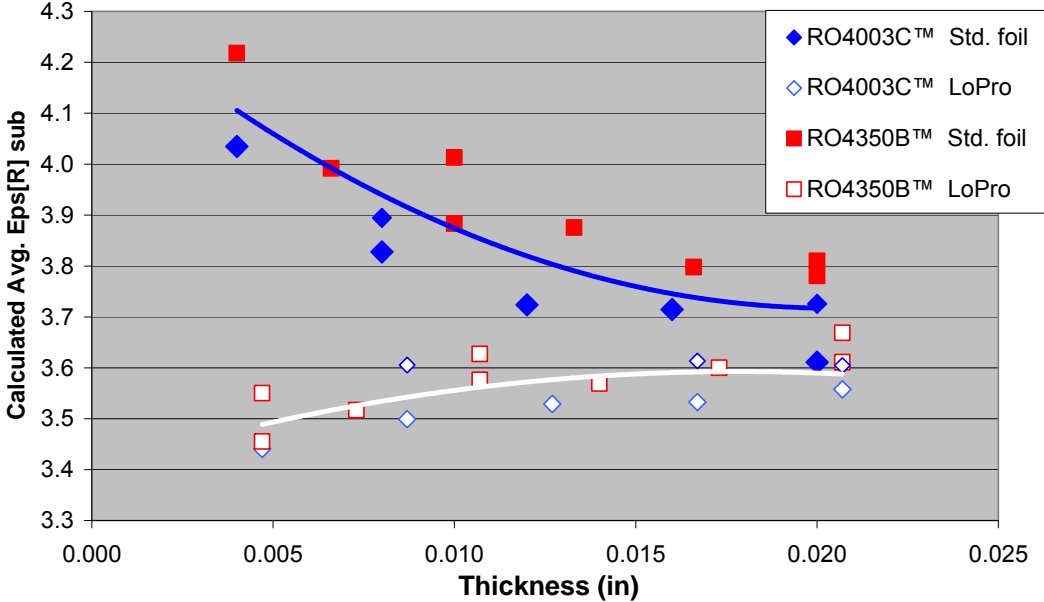
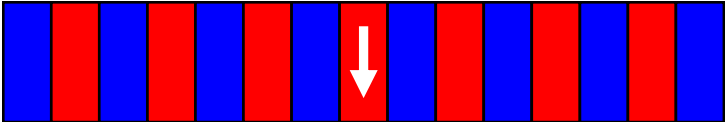
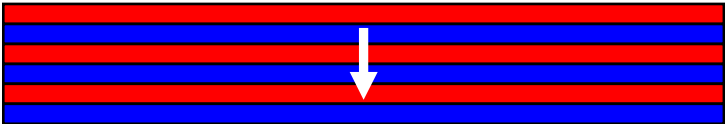


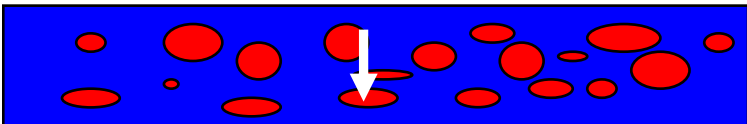
Figure 12. Data of reference 11



A – Parallel Arrangement



B – Series Arrangement



C – Dispersed Arrangement

Figure 13. Spatial arrangements of two-phase composite laminates

Dual Resonator - 12.5 GHz				
Laminate	IPC-TM-650 2.5.5.5 10 GHz	ϵ_{ZZ}	ϵ_{X-y}	ΔA (%)
RO3003™	3.00	2.97	3.00	1.0
RO3203™	3.00	2.96	3.18	7.2
NH9300	3.00	2.82	3.42	19.2
RO4003C™	3.38	3.37	3.66	8.3
NH9338	3.38	3.14	4.02	24.6
FR4	—	3.94	4.38	10.6
RO3010™	10.20	10.13	11.74	14.7
TMM® 10i	9.80	10.35	11.04	6.5

Table 3. Data of Dankov (reference 15)

RA Resonator - 8 GHz			
Laminate	Microstrip phase length ϵ_R 10 GHz	ϵ_{ZZ}	ϵ_{X-y}
FR4	4.3	4.06*	3.93*
RO4350B™	3.6	3.62	3.40
RO3010™	11.0	11.00	11.95

Table 4. Data of Rautio et al. (references 16 & 17)

* measured at 2 GHz

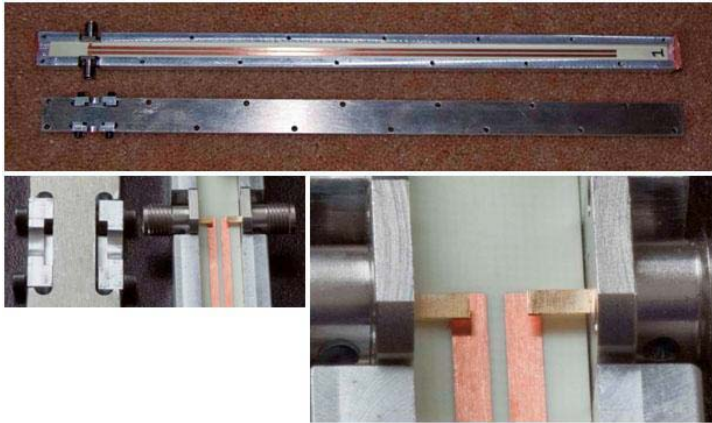


Figure 14. A 10 inch long RA resonator on Rogers RO4350B™ laminate, Lightly coupled at the ends via SMA connector tabs. The resonator is nearly 25λ at 16 GHz. (taken from reference 17)

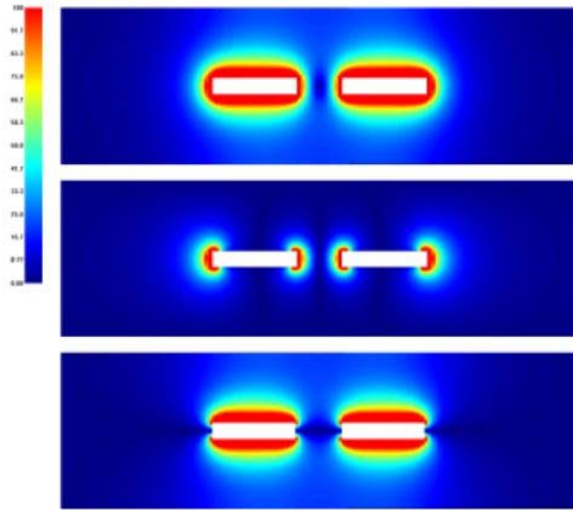


Figure 15a. Even mode \mathbf{E} -field of stripline coupled lines. Top image is total \mathbf{E} -field, center is magnitude of the in-plane component, and bottom is the magnitude of the z-axis component (taken from reference 16)

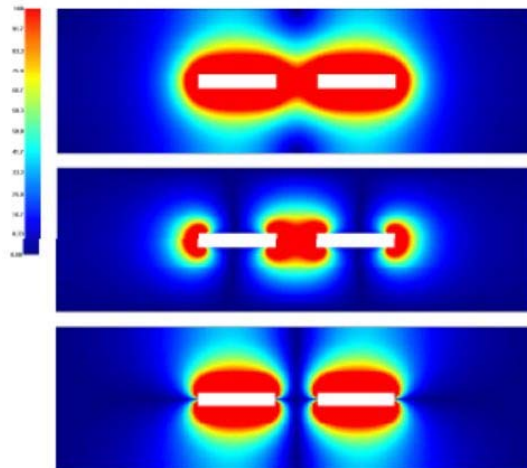


Figure 15b. Odd mode \mathbf{E} -field of stripline coupled lines. (taken from reference 16)